Developmental Biology 451 (2019) 68–78

Contents lists available at ScienceDirect

Developmental Biology

journal homepage: www.elsevier.com/locate/developmentalbiology

Rab11 is required for neurite pruning and developmental membrane protein degradation in *Drosophila* sensory neurons

Rafael Krämer, Sandra Rode, Sebastian Rumpf *

Institute for Neurobiology, University of Münster, Badestrasse 9, 48149, Münster, Germany

ARTICLE INFO

Keywords:
Dendrite
Ion channel
Rab11
Endocytosis
Pruning

ABSTRACT

Neurons, with their distinct neurites, require elaborate membrane trafficking pathways and regulation to uphold neurite identity and to be able to respond to neuronal or developmental stimuli. In a survey of trafficking regulators required for developmental dendrite pruning in *Drosophila* sensory neurons, we identified the small GTPase Rab11, a regulator of recycling endosomes. Dendrite pruning requires the developmentally regulated degradation of the cell adhesion molecule Neuroglian, and loss of Rab11 causes defects in the developmental degradation of Neuroglian and another target, the ion channel Ppk26. Rab11 often links vesicles to molecular motors, and we find that loss of the microtubule motor dynein also leads to defective Neuroglian and Ppk26 degradation. Loss of Rab11 also leads to defects in larval dendrite elaboration, and Neuroglian and Ppk26 localization is already altered at this stage. Our data highlight the importance of membrane protein recycling during development.

1. Introduction

Synapses, axons or dendrites can degenerate without loss of the parent neuron, and as a normal part of development, through a mechanism known as pruning. Pruning is used to ensure specificity of neuronal connections, and to remove developmental intermediates (Schuldiner and Yaron, 2015). In holometabolous insects, the nervous system is remodeled at a large scale during metamorphosis. In the peripheral nervous system (PNS) of *Drosophila*, several types of sensory neurons undergo either apoptosis or prune their larval processes in an ecdysone-dependent manner. The sensory class IV dendritic arborization (c4da) neurons completely and specifically prune their long and branched larval dendrites during the early pupal phase, while their axons stay intact (Kuo et al., 2005; Williams and Truman, 2005). C4da neuron dendrite pruning proceeds in a stereotypical fashion: at the onset of the pupal phase, ecdysone induces the expression of pruning factors such as Sox14 and Mical (Kirilly et al., 2009) as well as headcase (Loncle and Williams, 2012). Mical expression is also regulated at the level of mRNA translation (Rode et al., 2018). C4da neuron dendrites then thin out and eventually get severed at proximal sites close to the cell body between 5 and 10 h after puparium formation (h APF) in a manner that requires microtubule disruption (Herzmann et al., 2018, 2017). Severed dendrites are then fragmented and phagocytosed by the epidermal cells surrounding them (Han et al., 2014).

Membrane trafficking pathways play crucial roles during neuronal morphogenesis. Exocytic pathways provide membrane material during neurite growth (Ye et al., 2007). Both exo- and endocytic pathways regulate aspects like trafficking to specific neurites or surface exposure of transmembrane proteins such as cell adhesion molecules and ion channels. Differential trafficking of transmembrane receptors to axons or dendrites can occur by several distinct mechanisms (Lasiecka and Winckler, 2011). Some transmembrane receptors contain motifs that directly link them to motor proteins or cytoskeletal factors (Gu et al., 2006). Differential targeting also often involves a transcytosis-like mechanism where the transmembrane protein is first trafficked to the somatic cell surface and then endocytosed and recycled into vesicles that are capable of neurite-specific transport via association with specific motor proteins (Lasiecka and Winckler, 2011). Thus, endocytosis pathways play an important role in receptor trafficking to both axons and dendrites (Bentley and Banker, 2016; Farias et al., 2012). In addition, surface exposure of ion channels is often tightly regulated as a part of their functional regulation (Lau and Zukin, 2007).

Endocytosis and membrane protein degradation are also important for c4da neuron dendrite pruning. Several components of the endolysosomal pathway are required for pruning (Zhang et al., 2014; Loncle et al., 2015). The cell adhesion molecule Neuroglian (Nrg), the *Drosophila*

* Corresponding author.
E-mail address: sebastian.rumpf@uni-muenster.de (S. Rumpf).

https://doi.org/10.1016/j.ydbio.2019.03.003
Received 25 May 2018; Received in revised form 5 March 2019; Accepted 5 March 2019
Available online 11 March 2019

homologue of L1-CAM, seems to be a crucial endocytic substrate in this system (Zhang et al., 2014). Several motor proteins are also required for dendrite pruning, including kinesin-1 and kinesin-2 (Herzmann et al., 2018), and dynein (Lin et al., 2015) and it was recently shown that the kinesin-3 Unc-104 is required for Nrg degradation (Zong et al., 2018). Further prerequisites for receptor degradation, and how it is regulated during development, are still incompletely understood.

Here, we investigated the role of trafficking regulators during dendrite pruning. We found that the recycling endosome regulator Rab11 is required for c4da neuron dendrite pruning through a role in developmental Nrg degradation. We also identify the c4da neuron mechanosensory ENaC (endothelial sodium channel) channel Pickpocket 26 (Ppk26) as an additional substrate for developmental protein degradation. We also show that loss of the motor protein dynein causes similar defects during dendrite pruning and developmental membrane protein degradation as loss of Rab11. Rab11 is also required for proper c4da neuron dendrite elaboration at the larval stage, and our analyses suggest that Nrg and Ppk26 might be trafficked in a Rab11-dependent manner already at this stage. Thus, our results open up the possibility that developmental membrane protein degradation is linked to their exocytic trafficking.

2. Results

2.1. Rab11 is required for dendrite pruning

Endocytic membrane trafficking and membrane protein degradation has previously been shown to be important for c4da neuron dendrite pruning (Zhang et al., 2014; Loncle et al., 2015). In order to get more insight into the regulation of membrane trafficking during dendrite pruning, we assessed the effects of knocking down various Rab GTPases during this process (Fig. 1 A, B). From this analysis, the recycling endosome regulator Rab11 emerged as a prime candidate for a pruning regulator. In order to confirm these data, we first expressed an Orco (Odorant coreceptor) dsRNA construct in c4da neurons as a control. Such control c4da neurons have long and branched dendrites at the larval stage (Fig. 1 C) which are pruned completely during the first eighteen hours of the pupal phase (Fig. 1 D). Knockdown of Rab11 using two independent dsRNA lines targeting different regions of the Rab11 mRNA caused dendrite pruning defects with 30–60% of c4da neurons retaining one or two primary dendrite branches attached to the soma at 18 h after puparium formation (h APF) (Fig. 1 E, F, J, K). In order to confirm these results, we used MARCM (Mosaic Analysis with a Repressible Cell Marker) (Lee and Luo, 1999) to generate homozygous *rab11* mutant c4da neuron clones. While heterozygous *rab11*/+ control c4da neurons (in the same animals as the MARCM clones) did not display dendrite pruning defects (Fig. 1 G), c4da neurons homozygous for the strong loss-of-function alleles $rab11^{EP3017}$ and $rab11^{\Delta FRT}$ exhibited frequent dendrite pruning defects similar to the ones caused by RNAi-mediated knockdown (Fig. 1 H –K). We conclude that Rab11 is required for dendrite pruning.

2.2. Rab11 is required for Nrg degradation at the pupal stage

In order to explore the molecular basis for the dendrite pruning defects caused by loss of Rab11, we first asked whether Rab11 knockdown affects ecdysone-mediated gene expression. However, the ecdysone target genes headcase (Fig. 2 A, B), Sox14 (Fig. 2 C, D) and Mical (Fig. 2 E, F) were normally expressed in c4da neurons at the onset of the pupal phase upon Rab11 knockdown.

Endocytosis and lysosomal degradation of the cell adhesion molecule Nrg has been shown to be required for dendrite pruning (Wang et al., 2017; Zhang et al., 2014). We next asked whether loss of Rab11 also affects Nrg degradation. At the third instar larval stage, Nrg levels were similar in both controls and c4da neurons expressing *rab11* dsRNA (Fig. 3 A, A′, C, C′, G). At 6 h APF, Nrg levels were decreased in control neurons (Fig. 3 B, B′) as previously described (Zhang et al., 2014). In contrast, Nrg levels were more than twice as high at 6 h APF in c4da neurons expressing *rab11* dsRNA (Fig. 3 D, D', H, I). Similarly, c4da neuron MARCM clones homozygous for $rab11^{EP3017}$ showed much stronger Nrg staining at 6 h APF than heterozygous control c4da neurons in the same animals (Fig. 3 E − F). Thus, loss of Rab11 function interferes with Nrg degradation.

As Nrg degradation has been shown to be important for dendrite pruning, we next asked whether Nrg accumulation contributed to the pruning defects upon loss of Rab11. Downregulation of Nrg using dsRNA knockdown has been shown to partially suppress the pruning defects associated with the loss of several endocytic factors (Zhang et al., 2014). We therefore tested whether loss of Nrg would suppress the pruning defects upon loss of Rab11. To this end, we expressed dsRNA constructs targeting *orco* (as control), *rab11*, or *nrg* either alone or in combination. Neither Orco nor Nrg knockdown caused c4da neuron dendrite pruning defects at 18 h APF (Fig. 3 J, M) Expression of *rab11* dsRNA (either alone or in combination with *orco* dsRNA) caused fully penetrant dendrite pruning defects at 18 h APF (Fig. 3 K, M). These defects were stronger than those shown in Fig. 1, presumably because of the use of a different UAS-dcr2 construct for the dsRNA co-expression experiments. However, coexpression of *rab11* dsRNA with *nrg* dsRNA significantly reduced these pruning defects (Fig. 3 N), both at the level of penetrance and length of attached dendrites (Fig. 3 O, P). Taken together, these data suggest that a failure to degrade Nrg contributes to the pruning defects caused by the loss of Rab11.

2.3. Rab11 is required for developmental degradation of the ion channel Ppk26

In order to corroborate our observation that Rab11 is required for membrane protein degradation during developmental neurite pruning, we aimed to identify additional targets for this pathway. During our studies, we also assessed expression of the mechanosensory Epithelial Sodium Channel (ENaC) family ion channel Ppk26. This ion channel is specifically expressed in larval c4da neurons and contributes to their sensitivity to mechanical stimuli (Gorczyca et al., 2014; Guo et al., 2014; Mauthner et al., 2014). At the third instar larval stage, Ppk26 was readily detectable in the soma and neurites of c4da neurons and often displayed a partially dotted staining, likely reflecting vesicles (Fig. 4 A, A′). We next assessed Ppk26 levels at 6 h APF when Nrg is degraded (Zhang et al., 2014). At this stage, Ppk26 levels were significantly decreased (Fig. 4 B, B′, E). In order to assess whether Ppk26 is downregulated via a late endosomal/lysosomal degradation pathway, we expressed Shrub::GFP, an ESCRT-III subunit, in c4da neurons. This tagged version of Shrub acts in a dominant-negative fashion that inhibits ESCRT function (Sweeney et al., 2006), and causes c4da neuron dendrite pruning defects (Loncle et al., 2015). Shrub::GFP expression caused high levels of Ppk26 to persist at the pupal stage (Fig. 4 C – D', E). These data indicate that Ppk26 is degraded at the onset of the pupal phase through an ESCRT-dependent pathway.

We next assessed the effect of Rab11 knockdown on Ppk26 levels. Rab11 knockdown did not affect Ppk26 levels at the third instar larval stage compared to control neurons expressing *orco* dsRNA (Fig. 4 F, F′, H, H′, J). However, while control c4da neurons had again degraded most Ppk26 at 6 h APF (Fig. 4 G, G′, J), c4da neurons expressing *rab11* dsRNA still showed strong Ppk26 staining (Fig. 4 H–I', J). Thus, our results suggest that Rab11 function may be required broadly for developmental degradation of neuronal membrane proteins at the onset of the pupal stage.

2.4. Ppk26 and Nrg degradation during the pupal stage requires dynein

Rab11 often acts to recruit motor proteins to cargo vesicles (Welz et al., 2014). For example, the minus end-directed microtubule motor dynein mediates transport of Rab11 vesicles (Otani et al., 2011) and is

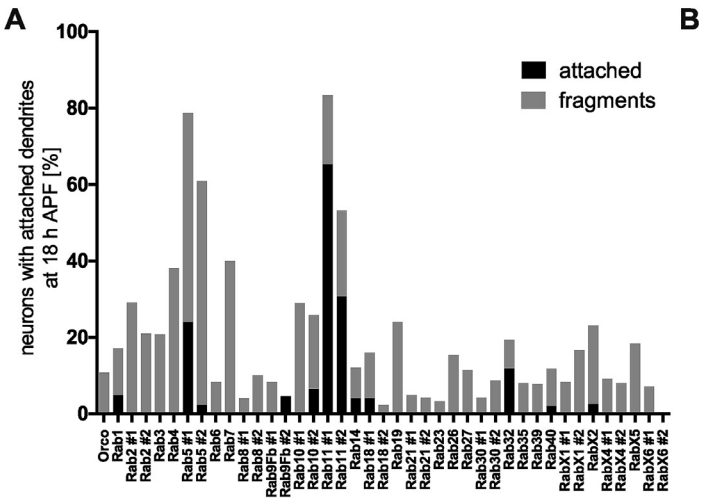

B

dsRNA	source	n	dsRNA	source	n
Orco	BL31279	364	Rab19	v103653	25
Rab1	BL27299	41	Rab21 #1	v109991	41
Rab2 #1	BL28701	31	Rab21 #2	v32940	24
Rab2 #2	v34767	62	Rab23	v13145	31
Rab3	v100787	24	Rab26	v101330	39
Rab4	v24672	21	Rab27	BL35774	53
Rab5 #1	v103945	75	Rab30 #1	v27002	48
Rab5 #2	v34096	87	Rab30 #2	v27004	46
Rab6	BL35744	24	Rab32	v104348	93
Rab7	v40337	70	Rab35	v101361	25
Rab8 #1	BL27519	25	Rab39	v31666	77
Rab8 #2	BL34373	40	Rab40	v110563	51
Rab9Fb #1	BL34374	24	RabX1 #1	BL28033	24
Rab9Fb #2	v102312	22	RabX1 #2	v103039	42
Rab10 #1	v28758	38	RabX2	v103311	39
Rab10 #2	v46792	31	RabX4 #1	BL28704	22
Rab11 #1	v22198	62	RabX4 #2	BL44070	25
Rab11 #2	v108382	72	RabX5	v103630	49
Rab14	v45774	25	RabX6 #1	BL26281	28
Rab18 #1	BL27665	25	RabX6 #2	BL53252	41
Rab18 #2	BL34734	43			

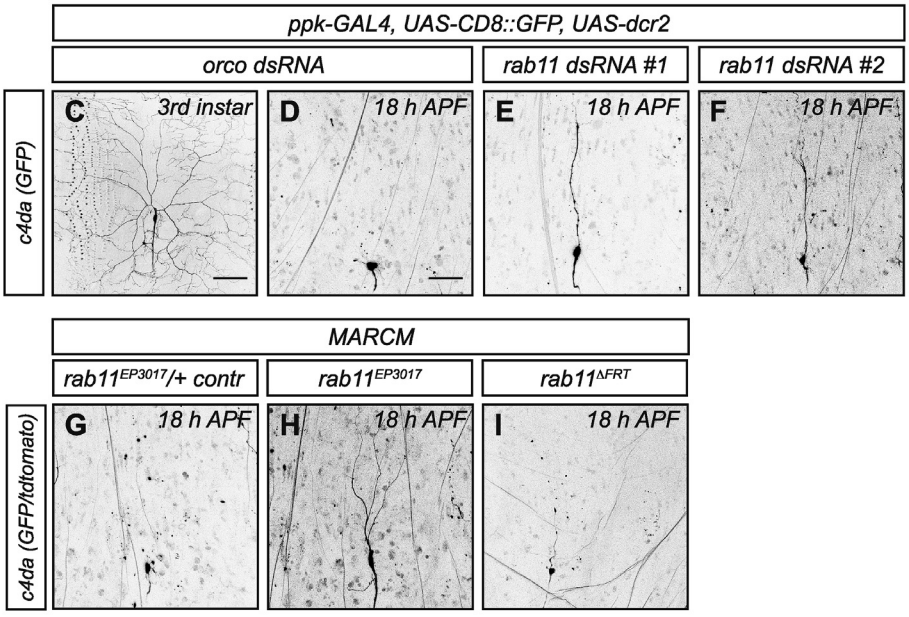

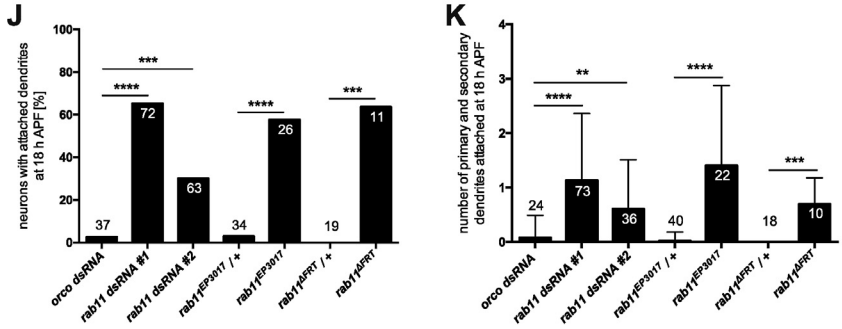

Fig. 1. Rab11 is required for c4da neuron dendrite pruning. **A** Graph depicting results from an RNAi screen for Rab GTPases required for c4da neuron dendrite pruning. dsRNA constructs targeting the mentioned Rab GTPases were expressed under ppk-GAL4, and effects on dendrite pruning of dorsal c4da neurons were assessed at 18 h APF. The penetrance of unpruned dendrites for each line is displayed in percent. **B** Table showing dsRNA lines used and N for each line. **C**–**I** Effects of loss of Rab11 on c4da neuron dendrite pruning. Neurons were labeled by *UAS-CD8GFP* expression under the control of *ppk-GAL4* (**C**–**F**), by a *ppk-eGFP* promotor fusion (**G**), or by tdtomato expression in c4da neuron MARCM clones (**H**, **I**). **C** Control third instar larval c4da neuron with long and branched dendrites. **D** Control c4da neuron at 18 h APF has pruned all larval dendrites. **E** A c4da neuron expressing *rab11* dsRNA #1 (VDRC 22198) retains larval dendrites at 18 h APF. **F** C4da neuron expressing *rab11* dsRNA #2 (VDRC 108382) at 18 h APF. **G** Heterozygous $rab11^{EP3017}$/+ c4da neuron labeled with *ppk-eGFP* at 18 h APF. **H** Homozygous $rab11^{EP3017}$ c4da MARCM clone labeled by tdtomato at 18 h APF. **I** Homozygous $rab11^{\Delta FRT}$ c4da MARCM clone labeled by tdtomato at 18 h APF. **J** Penetrance of dendrite pruning defects in **D** – **I** in %. ***P < 0.001, ****P < 0.0001 (using Fisher's exact test). **K** Number of attached primary and secondary dendrites at 18 h APF in **D** – **I** as a measure of severity. Data are mean±SD, **P < 0.01, ***P < 0.001, ****P < 0.0001 (using Wilcoxon's test). N is indicated in the graph. Scale bars in **C** and **D** are 100 and 50 μm, respectively.

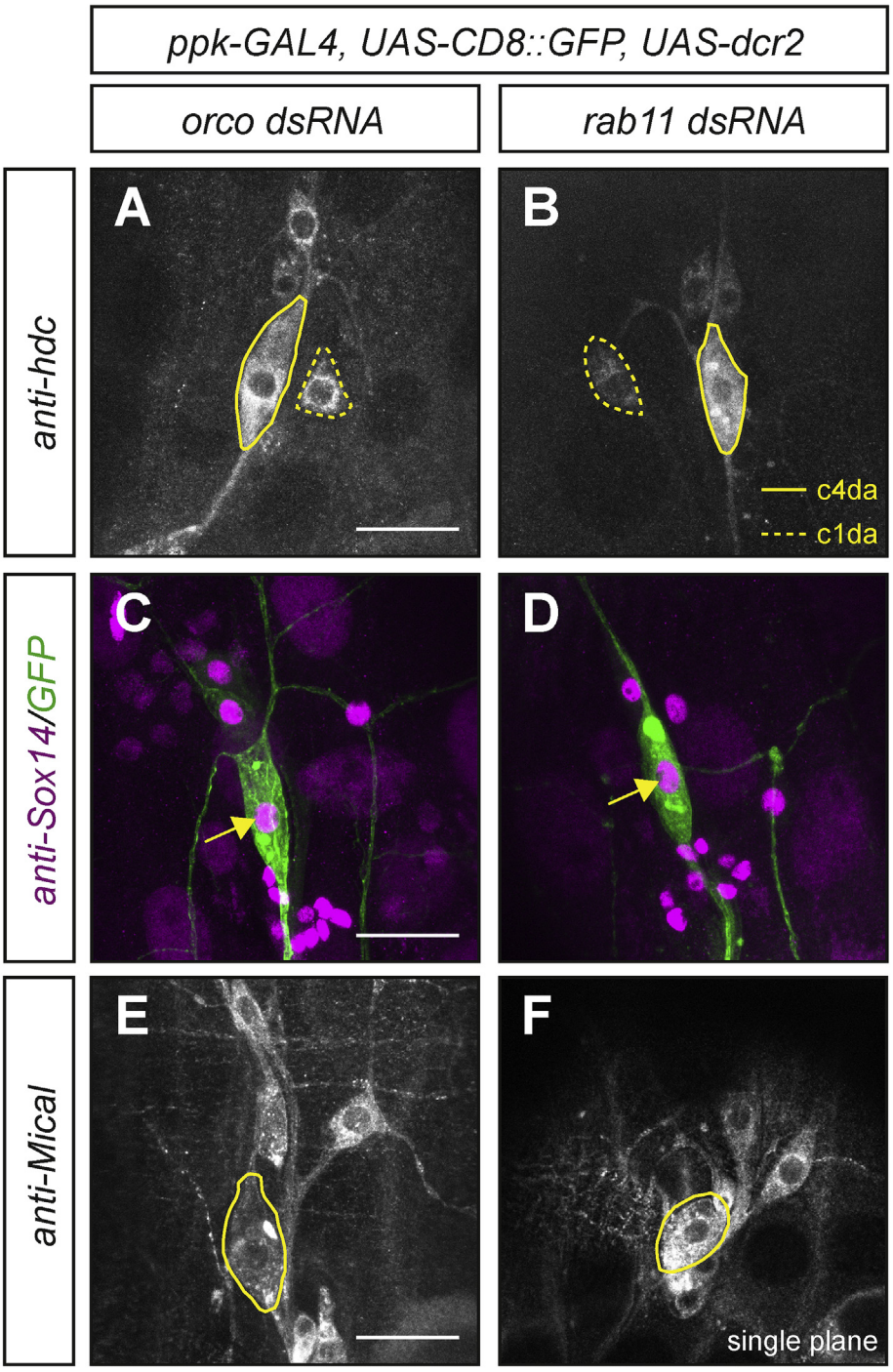

Fig. 2. Rab11 knockdown does not affect expression of ecdysone target genes in c4da neurons. **A**, **B** headcase expression in control c4da neurons (**A**) or in c4da neurons expressing *rab11* dsRNA (**B**) at 2 h APF. C4da neuron cell bodies are marked by continuous lines, the cell bodies of adjacent non-manipulated c1da neurons (for comparison) are marked by dotted lines.
C, **D** Sox14 expression in control c4da neurons (**C**) or in c4da neurons expressing *rab11* dsRNA (**D**) at 2 h APF. Sox14 staining is shown in magenta, c4da neurons are labeled by GFP (green).
E, **F** Mical expression in control c4da neurons (**E**) or in c4da neurons expressing *rab11* dsRNA (**F**) at 2 h APF. C4da neuron cell bodies are marked by continuous lines.
Scale bars are 20 μm.

required for larval c4da neuron dendrite morphogenesis (Arthur et al., 2015; Satoh et al., 2008; Zheng et al., 2008). Interestingly, several motors are required for c4da neuron dendrite pruning, including dynein (Lin et al., 2015), kinesin-1 and kinesin-2 (likely through a role in microtubule organization) (Herzmann et al., 2018) and kinesin-3 (through a role in Nrg degradation) (Zong et al., 2018). To address whether kinesin-1 and dynein, two known Rab11 interactors, are also involved in developmental membrane protein degradation during c4da neuron dendrite pruning, we knocked down *khc* (encoding the kinesin-1 motor subunit) or *dlic*, encoding the essential dynein light intermediate chain. We confirmed that Khc and Dlic knockdown caused significant c4da neuron dendrite pruning defects at 18 h APF (Fig. 5 A – E). We next assessed the effects of *khc* and *dlic* dsRNA expression on Nrg levels. Nrg was mostly degraded at this stage in control c4da neurons (Fig. 5 F, F′), and it was apparently also normally degraded upon Khc knockdown (Fig. 5 G, G′, K). However, *dlic* dsRNA expression caused a significant increase in Nrg levels (Fig. 5 H, H′, K). Similarly, Ppk26 levels at 6 h APF were increased upon *dlic* dsRNA (Fig. 5 I - J', L). Thus, developmental membrane protein degradation in c4da neurons seems to depend on a specific subset of motor proteins.

2.5. Loss of Rab11 affects dendrite morphogenesis in larval c4da neurons

Given that the function of Rab11 is the regulation of recycling endosome function and exocytosis of recycled membrane proteins, we also wanted to assess the effects of loss of Rab11 on dendrite elaboration at

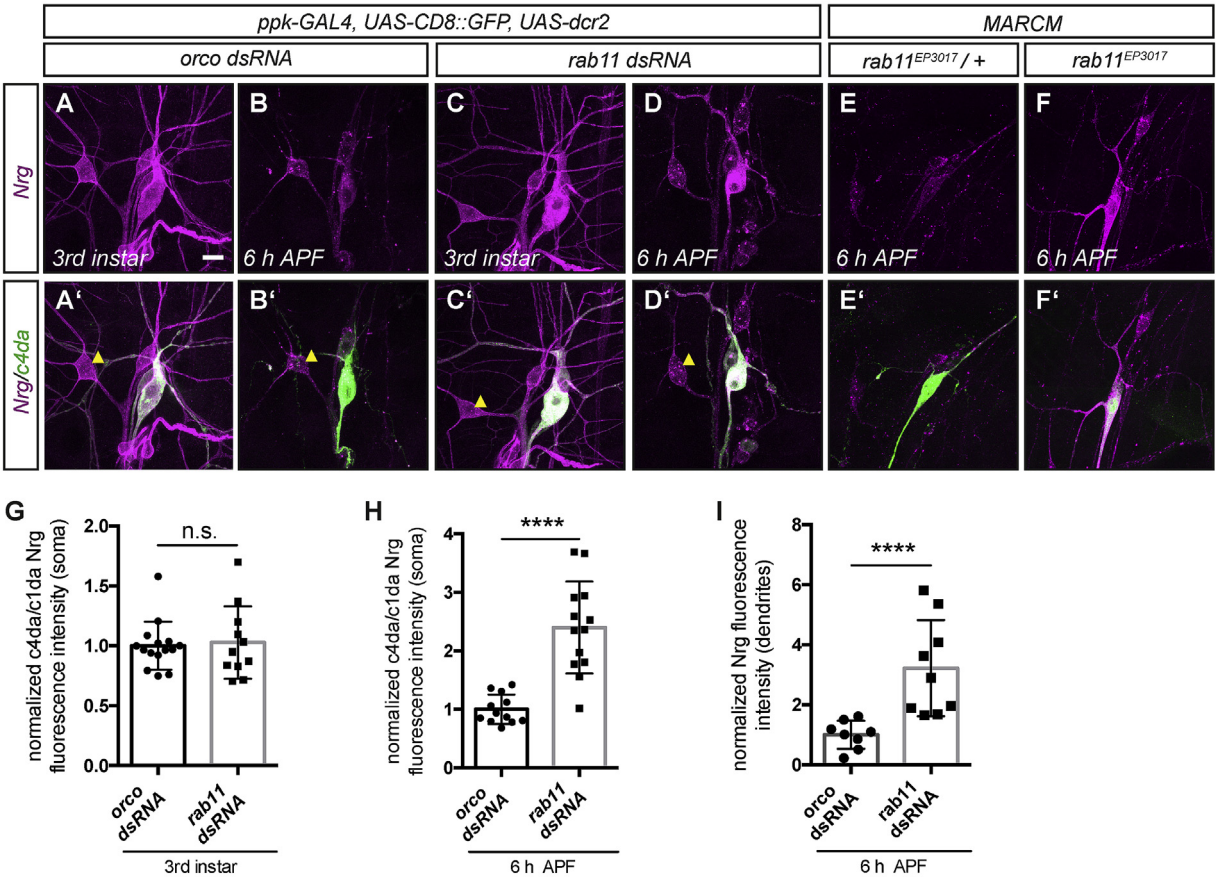

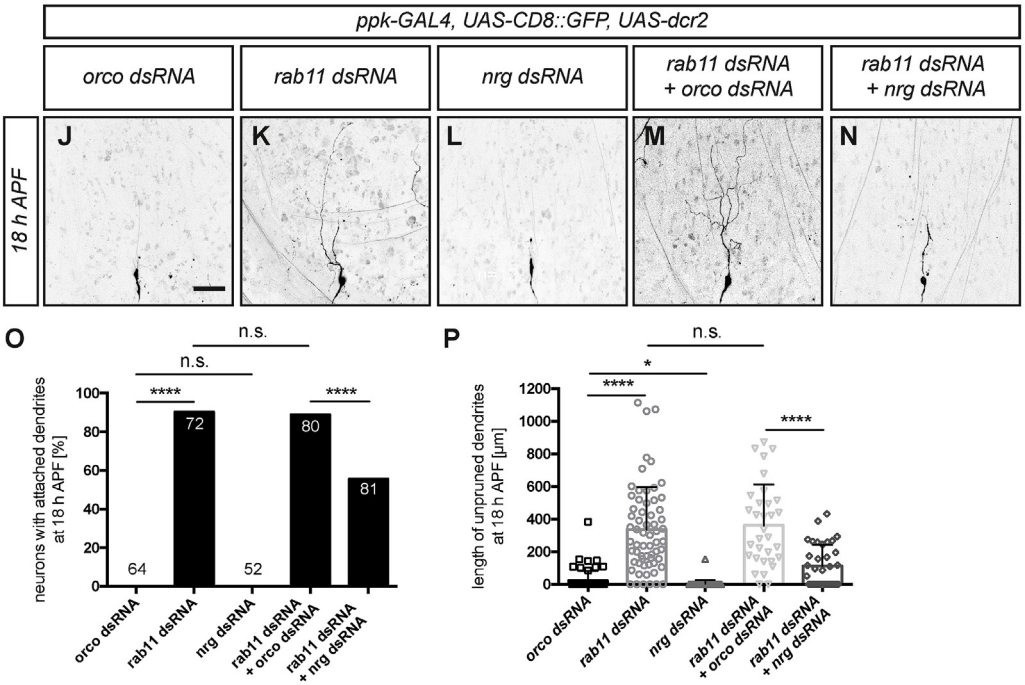

(caption on next page)

Fig. 3. Rab11 affects Nrg degradation.
A – F′ Upper panels (**A–F**) show Nrg stainings using the BP104 antibody, lower panels (**A' – F′**) show the merge with the GFP or tdtomato (false-colored in green) markers labeling c4da neurons.
A - B′ control c4da neurons expressing CD8::GFP under the control of *ppk-GAL4* at the third instar larval stage (**A**, **A′**) or at 6 h APF (**B**, **B′**).
C - D′ C4da neurons expressing *rab11 ds*RNA under *ppk-GAL4* at the third instar larval stage (**C**, **C′**) or at 6 h APF (**D**, **D′**).
E, **E′** heterozygous $rab11^{EP3017}/+$ control c4da neuron labeled with *ppk-eGFP* at 6 h APF.
F, **F′** homozygous $rab11^{EP3017}$ c4da neuron MARCM clone labeled with tdtomato at 6 h APF.
G- I quantification of Nrg staining intensity in third instar c4da neurons (**G**) or at 6 h APF (**H**, **I**). For quantification of Nrg staining intensity in the soma of control c4da neurons or c4da neurons expressing *rab11* dsRNA was normalized against staining intensity of adjacent c1da neurons (marked by triangles in panels **A'** – **D′**) and compared using Wilcoxon's test. Data are mean±SD, ****P < 0.0001. **I** Nrg staining intensity in proximal dendrites of samples shown in panels **B** and **D** was measured as described under Methods, and compared using Wilcoxon's test. Data are mean±SD, ****P < 0.0001. **J - P** genetic interactions between Rab11 and Nrg. **J** C4da neuron expressing *orco* dsRNA at 18 h APF. **K** C4da neuron expressing *nrg* dsRNA at 18 h APF. **L** C4da neuron expressing *rab11* dsRNA at 18 h APF. **M** C4da neuron coexpressing *rab11* and *orco* dsRNA constructs at 18 h APF. **N** C4da neuron coexpressing *rab11* and *nrg* dsRNA constructs at 18 h APF. **O** quantification of the penetrance of the pruning defects in **J - N**. ****P < 0.0001 (using Fisher's exact test). **P** quantification of the length of unpruned dendrites in **J - N**. Data are mean±SD, *P < 0.05, ****P < 0.0001 (using Wilcoxon's test). Scale bars are 10 and 50 μm in **A** and **J**, respectively.

the larval stage. At this stage, control c4da neurons have long and highly branched dendrites (Fig. 6 A). We used Sholl analysis to count the number of dendrite branch intersections with concentric rings around the soma as a measure of dendrite elaboration (Fig. 6 C). We first assessed c4da neurons expressing Orco dsRNA as controls. These neurons cover the whole segment area with their dendrites (Fig. 6 A) and showed a peak of approximately 80 intersections at a distance of 250 μm from the soma (Fig. 6 C). In contrast, c4da neurons expressing Rab11 dsRNA did not cover the whole segment area (Fig. 6 B) and showed a peak of approximately 35 intersections at a distance of 220 μm from the soma (Fig. 6 C), indicating a strong loss of higher order dendrite branches compared to the control. Thus, Rab11-mediated membrane traffic is also important for dendrite growth.

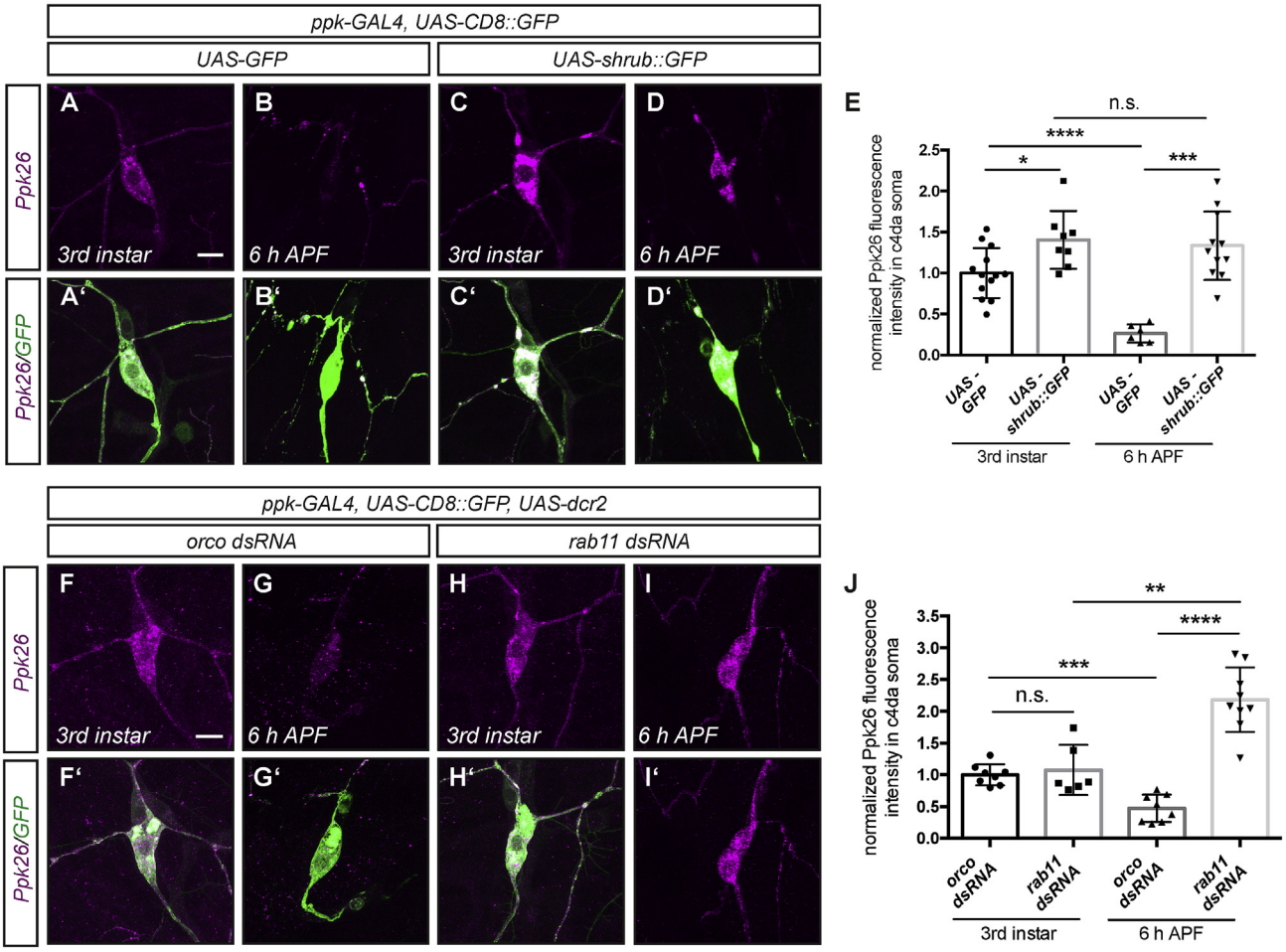

Fig. 4. Ppk26 is degraded during the early pupal stage in an ESCRT-III and Rab11-dependent manner. C4da neurons were labeled by CD8::GFP driven by *ppk-GAL4*, and Ppk26 was visualized by immunofluorescence with a Ppk26 antibody. Panels **A–D** and **F –I** show Ppk26 stainings, panels **A' – D′**, **F' – I′** show merge with GFP. **A – E** Developmental Ppk26 degradation. Ppk26 was stained in control animals at the third instar larval stage (**A**, **A′**) or at 6 h APF (**B**, **B′**). **C**, **D** Ppk26 staining in animals expressing dominant-negative Shrub::GFP at the third instar (**C**, **C′**) or at 6 h APF (**D**, **D′**). **E** Quantification of normalized Ppk26 staining intensities in panels **A–D**. Data are mean±SD, *P < 0.05, ***P < 0.001, ****P < 0.0001 using Wilcoxon's test. **F–I′** Rab11 is required for Ppk26 degradation. Ppk26 was stained in control animals at the third instar larval stage (**F**, **F′**) or at 6 h APF (**G**, **G′**), or in animals expressing *rab11* dsRNA in c4da neurons at the third instar (**H**, **H′**) or at 6 h APF (**I**, **I′**). **J** Quantification of normalized Ppk26 staining intensities in panels **F –I**. Data are mean±SD, **P < 0.01, ***P < 0.001, ****P < 0.0001 using Wilcoxon's test. Scale bars in **A** and **F** are 10 μm.

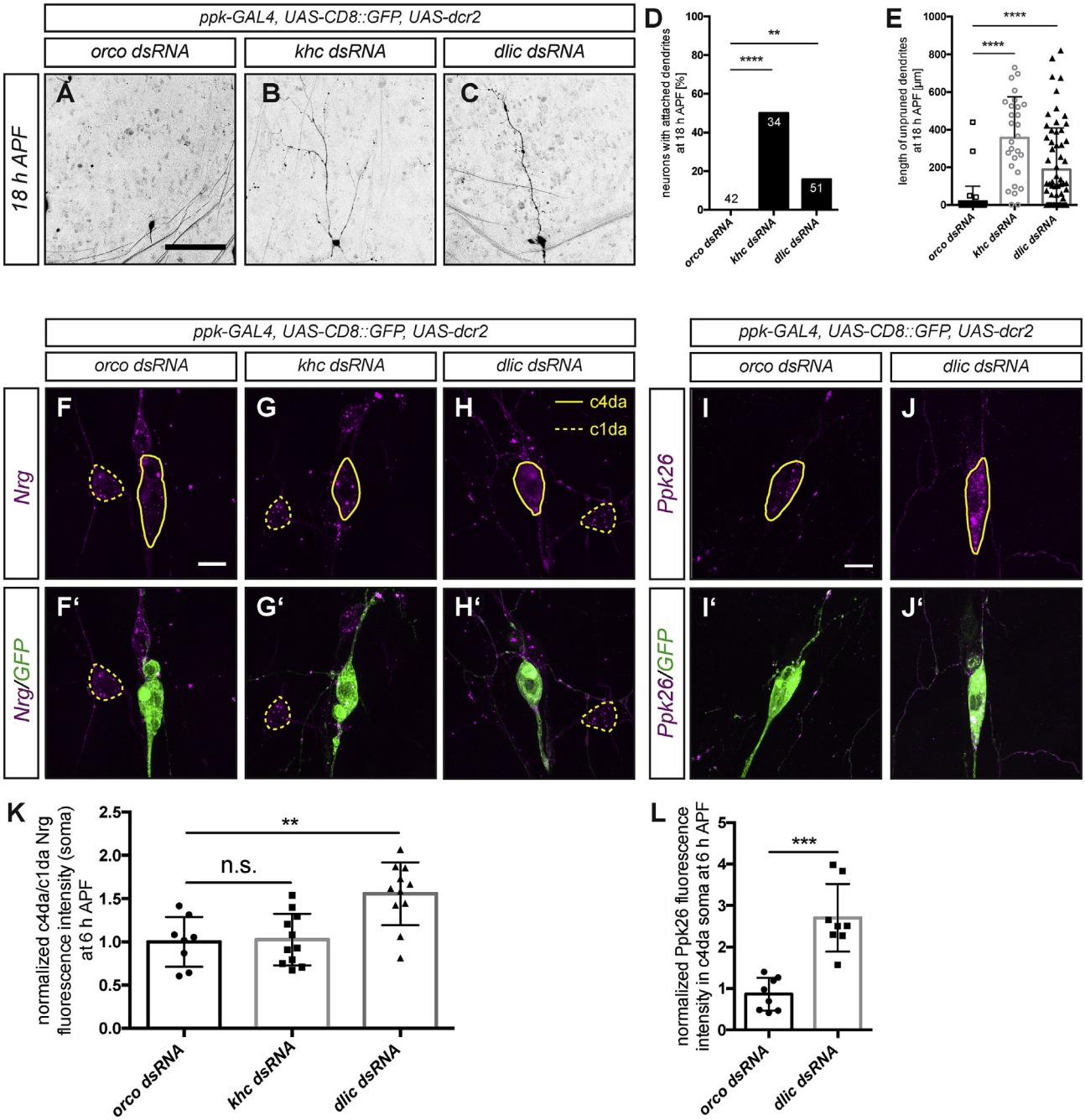

Fig. 5. Dynein light intermediate chain is required for Ppk26 and Nrg degradation. A – E Dlic and Khc are required for c4da neuron dendrite pruning. **A** C4da expressing *orco* dsRNA at 18 h APF. **B** C4da expressing *khc* dsRNA at 18 h APF. **C** C4da neuron expressing *dlic* dsRNA at 18 h APF. **D, E** Quantification of c4da neuron dendrite pruning defects in panels **A–C**. **D** Penetrance of dendrite pruning defects. **P < 0.01, ****P < 0.0001 (using Fisher's exact test). **E** Length of attached dendrites at 18 h APF as a measure of severity. Data are mean±SD, ****P < 0.0001 (using Wilcoxon's test). **F–H′** Dlic, but not Khc, is required for Nrg degradation. Upper panels (**F–H**) show Nrg stainings, and lower panels (**F' – H′**) show the merge with the GFP marker labeling c4da neurons. **I – J′** Developmental Ppk26 degradation requires Dlic. Ppk26 was stained at 6 h APF in control animals (**I, I′**) or in animals expressing *dlic* dsRNA under *ppk-GAL4* (**J, J′**). **K** Quantification of Nrg levels in **F–H** was done as in Fig. 3. **L** Quantification of Ppk26 levels in **I - J** was done as in Fig. 4. Statistical analysis was done using Wilcoxon's test (**P < 0.01, ***P < 0.001). Scale bars are 100 µm in **A** and 10 µm in **F** and **I**.

2.6. Effects of Rab11 knockdown on Nrg and Ppk26 at the larval stage

To further assess the role of Rab11 in larval c4da neurons, we next asked whether Rab11 knockdown also affects the distribution of Nrg and Ppk26 at this stage. To this end, we assessed whether Nrg colocalizes with recycling endosomes marked by GFP-tagged human transferrin receptor (hTfR::GFP). At the third instar stage, Nrg was mostly evenly distributed across the soma of control c4da neurons, and only very few punctate structures could be seen (Fig. 7 A). hTfR::GFP, on the other hand, localized mostly to punctate vesicular structures in the soma of c4da neurons, with apparent diameters of 0.3–1 µm (Fig. 7 A′). Importantly, there was no overlap between hTfR::GFP vesicles and Nrg punctae in control neurons (Fig. 7 A′, C). Upon Rab11 knockdown, punctate structures could be observed more frequently in Nrg stainings in addition to the normal even distribution (Fig. 7 B). These Nrg-positive punctae were relatively large (apparent diameter around 1 µm) and consistently

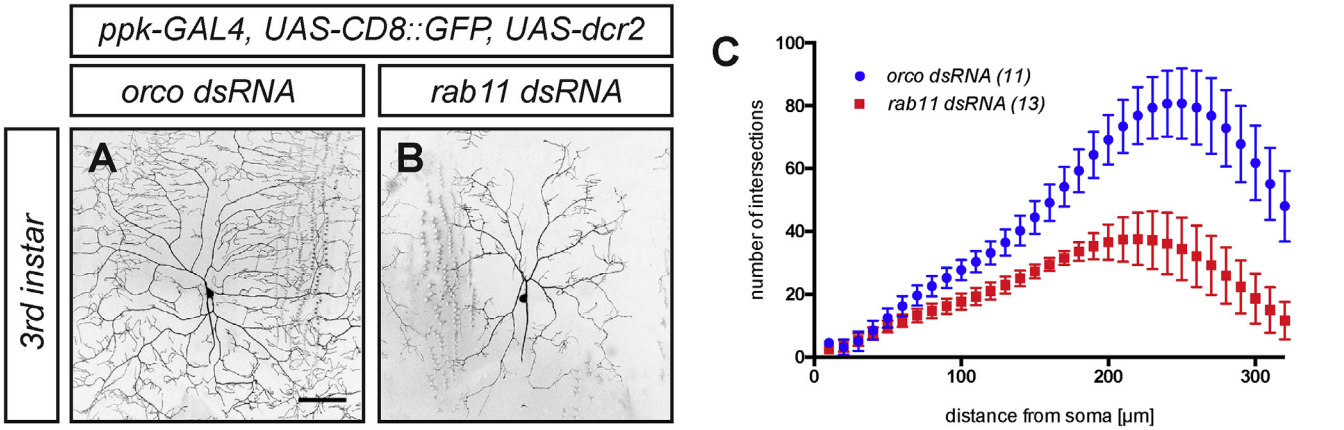

Fig. 6. Rab11 is required for normal dendrite elaboration of larval c4da neurons. Wandering third instar larval c4da neurons were labeled by CD8::GFP expression under the control of *ppk-GAL4*. **A** Control c4da neuron expressing *orco* control dsRNA. **B** C4da neuron expressing *rab11* dsRNA. **C** Sholl analysis of dendrite arbors of c4da neurons in **A** and **B**. N is indicated in the graph. The scale bar in A is 100 µm.

also positive for hTfR::GFP (Fig. 7 B, B', C). These data are consistent with the idea that some Nrg becomes trapped in recycling vesicles, possibly at some point during its biogenesis.

In order to assess the effects of Rab11 on Ppk26 in larval c4da neurons, we next generated a UAS-Dendra2::Ppk26 transgene. We then used *ppk-GAL4* to express Dendra2::Ppk26 in c4da neurons. Consistent with previous results (Mauthner et al., 2014), fluorescently tagged Ppk26 was seen in the soma and dendrites of c4da neurons both in punctate vesicular structures and also following the contours of the cell body and dendrites, suggestive of plasma membrane localization (Fig. 7 D, E). Stochastic expression of the used *ppk-GAL4* insertion line in class 3 da (c3da) neurons also allowed us to visualize Dendra2::Ppk26 in these neurons. Consistent with previous results (Mauthner et al., 2014), Dendra2::Ppk26 was only seen in punctate vesicular structures in this neuronal subtype, but to a much lower degree evenly around the cell contours (Fig. 7 D), likely because c3da neurons do not express the Ppk26 binding partner Ppk1, thus preventing plasma membrane targeting (Mauthner et al., 2014). We next assessed the effects of Rab11 knockdown on Dendra2::Ppk26 distribution in c4da neurons. Interestingly, we consistently observed that Dendra2::Ppk26-positive vesicles appeared larger and more clustered in c4da neurons expressing *rab11* dsRNA (n = 11 each). Thus, trafficking of both Nrg and Ppk26 might be altered by Rab11 knockdown at the larval stage. Taken together, our results suggest that Rab11 could be involved in distinct trafficking steps for Nrg and Ppk26 during different developmental stages.

3. Discussion

In this study, we investigated the roles of Rab GTPases during dendrite pruning in *Drosophila* PNS neurons. We found that Rab11, a known regulator of recycling endosomes and exocytosis, is required for c4da neuron dendrite pruning. Surprisingly, we found that Rab11 is required for the developmental degradation of two neuronal membrane proteins at the onset of the pupal phase, the cell adhesion molecule Nrg and the mechanosensory ion channel Ppk26. The impaired degradation and persistence of Nrg at the pupal phase together with our genetic data showing a partial suppression of the Rab11 pruning phenotype suggest that this defect in membrane protein degradation underlies at least in part the observed pruning defects.

We further show that Rab11 is needed for normal elaboration of PNS neuron dendrites at the larval stage, and that it might affect trafficking of Nrg and Ppk26 already at this stage. Specifically, Rab11 downregulation led to an increased localization of Nrg to putative recycling compartments in the soma of c4da neurons, and to a change in the appearance of Ppk26-containing vesicles. While these changes are relatively subtle and the distributions of both these membrane proteins still seem relatively similar to controls, these data suggest that Rab11 might contribute to their trafficking also at this stage.

How could Rab11 be involved in Ppk26 and Nrg degradation at the pupal stage? We envisage two potential mechanisms for this. Firstly, loss of Rab11 could indirectly affect the maturation of early endosomes into late endosomes and thus prevent membrane protein degradation. In support of this idea, the early endosome regulator Rab5 is known to be required for membrane protein degradation and dendrite pruning in c4da neurons (Zhang et al., 2014; Kanamori et al., 2015). Alternatively, it is interesting to speculate that Nrg and Ppk26 degradation could be linked to their initial membrane targeting, e. g., they could be degraded more efficiently if they are targeted to the membrane in a Rab11-dependent manner. In line with this idea, it was recently shown that loss of exocytic Golgi proteins also leads to defects in developmental Nrg degradation and c4da neuron dendrite pruning (Wang et al., 2017, 2018).

A potential role for Rab11 during large-scale pruning has previously been assessed during mushroom body γ neuron axon pruning (Issman--Zecharya and Schuldiner, 2014). Surprisingly, and in contrast to dendrite pruning, Rab11 does not seem to be required in that system. It is interesting to speculate that this differential requirement might reflect a difference in axonal versus dendritic membrane protein trafficking and degradation, rather than a specific feature of the systems studied.

Lastly, the observation that Ppk26 is degraded at the onset of the pupal phase suggests that c4da neurons reduce their excitability (in this case, to harsh touch) during the pupal phase. In support of this idea, transcriptional profiling of mushroom body neurons has also shown that neuronal ion channels are downregulated during the pupal stage (Hoopfer et al., 2008). It will be interesting to see whether Ppk26 expression is only transiently downregulated, or whether it is permanently shut down to allow for the acquisition of new functional properties in the adult. Taken together, our data provide new insights into the function of Rab11 during neuronal development and differentiation.

4. Materials and methods

4.1. Fly stocks and culture

All crosses were done at 25 °C under standard conditions. For expression in c4da neurons, we used *ppk-GAL4* insertions on the second and third chromosomes (Grueber et al., 2007). The alleles $Rab11^{EP3017}$ (BL #42708) and $Rab11^{\Delta FRT}$ (Bogard et al., 2007) were recombined with FRT82B. MARCM clones were induced with *SOP-FLP* (Matsubara et al., 2011) and labeled by UAS-tdtomato (Han et al., 2014) expression under $GAL4^{109(2)80}$ (Gao et al., 1999). For better identification of c4da neurons

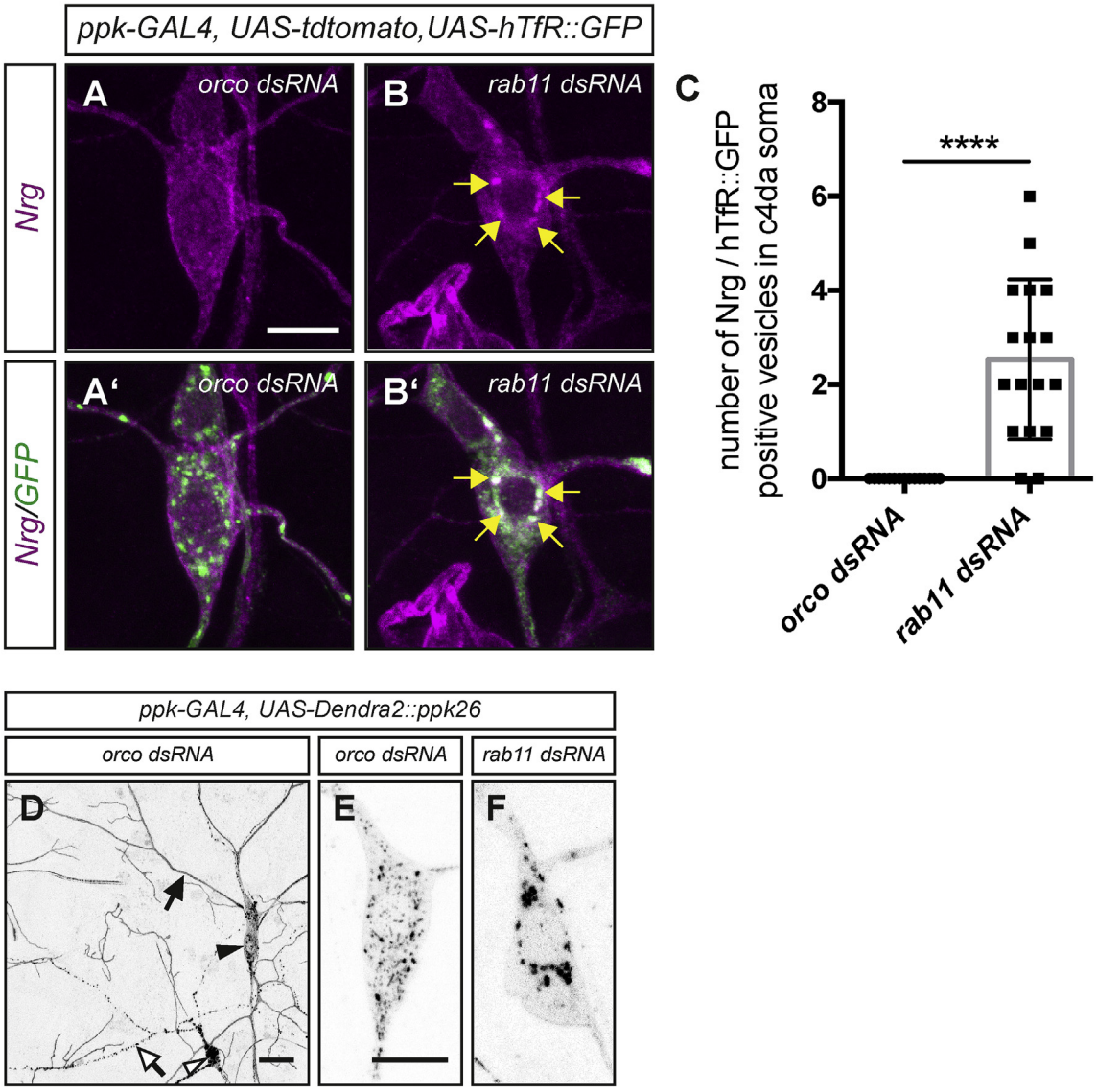

Fig. 7. Effect of Rab11 knockdown on Nrg and Ppk26 subcellular distribution. **A** – **C** Effects of Rab11 knockdown on Nrg colocalization with hTfR::GFP. Upper panels show Nrg stainings of larval filets (**A**–**B**), lower panels (**A'** – **B'**) show the merge with hTfR::GFP expressed under *ppk-GAL4*. **A**, **A'** C4da neuron expressing *orco* dsRNA. **B**, **B'** C4da neuron expressing *rab11* dsRNA. **C** Quantification of hTfR::GFP- and Nrg-double positive dot structures in **A** and **B**. Data are mean±SD, ****P < 0.0001 using Wilcoxon's test. **D** Distribution of Dendra2::Ppk26 expressed in c4da and c3da neurons under *ppk-GAL4*. C4da and c3da neuron somata are indicated by filled and open arrowheads, respectively, c4da and c3da neuron dendrites are indicated by filled and open arrows. **E** – **F** Rab11 knockdown affects Dendra2::Ppk26-positive vesicles in the c4da neuron soma. Close-up views of c4da neuron soma of neurons expressing *orco* dsRNA (**E**) or *rab11* dsRNA (**F**). N = 11 for each genotype. Scale bars are 10 μm in **A** and **E,** and 20 μm in **D**.

and for use of heterozygous neurons as internal control, our MARCM line also contains the marker *ppk-eGFP* (Grueber et al., 2003). For *rab11* genetic interactions, candidates were crossed to a stock carrying *ppk-GAL4* combined with *UAS-CD8GFP*, *UAS-dcr2* (2nd *chromosome*) and *UAS--rab11 dsRNA* #1 (VDRC #22198) (3rd chromosome). Other Rab dsRNA lines are mentioned in Fig. 1 B.

Other fly lines were UAS-GFP (BL #1521), UAS-hTfR::GFP (BL #36858), UAS-dcr2 insertions on the second and third chromosomes (Dietzl et al., 2007), UAS-shrub::GFP (Sweeney et al., 2006). UAS-dsRNA lines were: *rab11* (VDRC #22198 (dsRNA #1, used unless indicated differently), VDRC #108382 (dsRNA #2)), *nrg* (VDRC #27202), *khc* (NIG 7765R-1), *dlic* (VDRC #101340). *orco* dsRNA (BL #31279) was used as control in all RNAi experiments. UAS-Dendra2::Ppk26 was cloned into pUAST attB according to standard procedures and injected into flies carrying the 86Fb insertion site (Bischof et al., 2007).

4.2. Dissection, microscopy and live imaging

Pruning defects were assayed at 18 h APF as described (Rumpf et al., 2014) and analyzed using a Nikon AZ100 dissecting microscope or Zeiss LSM710 confocal microscope. Immunostainings were imaged using a Zeiss LSM880 confocal microscope. For *rab11* genetic interactions, candidates were crossed to a second chromosome insertion of *ppk-GAL4* combined with *UAS-CD8GFP, UAS-dcr2* and *UAS-rab11 dsRNA* #1. Images were obtained with ZEN software (Zeiss) and processed in ImageJ (Schindelin et al., 2012). Pruning phenotypes were analyzed by counting the number of neurons that still had dendrites attached to the soma (as a measure of phenotypic penetrance), these data were analyzed using a two-tailed Fisher's exact test. As a measure of severity, we used the added numbers of attached primary and secondary dendrites at 18 h APF or the mean length of remaining dendrites at 18 h APF (measured using the ImageJ plugin NeuronJ (Meijering et al., 2004)). These data were

analyzed using the Wilcoxon-Mann-Whitney test.

4.3. Antibodies and immunohistochemistry

Larval or pupal filets were dissected according to standard protocols and fixed in PBS containing 4% formaldehyde.

Primary antibodies used were mouse anti-Nrg180 (BP104, DSHB), rabbit anti-Ppk26 (gift from Yuh Nung Jan, Gorczyca et al., 2014), chicken anti-GFP (Aves labs), rabbit anti-DsRed (Clontech), guinea pig anti-Sox14 (Ritter and Beckstead, 2010), mouse anti-hdc (HDC U33, DSHB) and anti-HRP (Alexa Fluor 647 conjugated, Dianova), rabbit anti-Mical (Rode et al., 2018). Secondary antibodies used were Alexa Fluor 488/568/647 (Molecular Probes).

4.4. Image analysis and quantification

For all quantifications, only c4da neurons in the dorsal cluster (ddaC) were assessed.

For quantification of Nrg levels in the soma, ratios of the pixel intensities of c4da da and c1da (ddaD or ddaE of the same cluster) were calculated. C1da neurons were not affected by the manipulations. For dendrites, intensity values were measured along similar stretches of proximal dendrites and background was subtracted. Integrated density values were used for the calculations to correct for differences in area. To measure intensities, a maximum intensity projection (MIP) was generated, and the c4da soma ROI was selected according to the GFP channel. The adjacent c1da soma ROI was selected according to HRP staining. The obtained ratios were normalized to the respective control. For Ppk26 immunostaining quantification, background was subtracted from the stacks (rolling ball radius = 100), a maximum projection was generated, and the pixel intensity (integrated density) in the c4da soma (ROI selected according to GFP channel) was measured and normalized to controls.

For analysis of larval dendrites, binary images were generated using gamma correction (0.5) and background subtraction (rolling ball radius = 2) in stacks followed by generation of a maximum intensity projection. Somata and axons were manually removed in Fiji using the brush tool. Sholl analysis was performed on these images using the Fiji Sholl analysis plugin v3.7.4 (Ferreira et al., 2014).

Colocalization of Nrg with hTfR::GFP was defined as overlapping punctate structures of similar size (0.3–1 μm) and shape in both the Nrg and GFP stainings under nonsaturating conditions.

Graphs and quantifications were performed using Excel (Microsoft) and Prism (GraphPad). Asterisks in graphs refer to following P-Values (*$P \leq 0.05$, **$P < 0.01$,***$P < 0.001$, ****$P < 0.0001$).

Author contributions

RK and S. Rumpf designed and conceived the project and interpreted the data. RK, S. Rode and S. Rumpf performed experiments. RK and S. Rumpf contributed reagents. S. Rumpf wrote the manuscript with help from RK.

Conflicts of interest

The authors declare that they have no conflict of interest.

Acknowledgements

We are grateful to C. Klämbt for generous support, to C. Klämbt for helpful comments on the manuscript, and to M. Galic and S. Luschnig for discussions. We thank J. Kauffmann for help with UAS-Dendra2::Ppk26 cloning and S. Herzmann for the khc RNAi data, and C. Klämbt, Y. Jan, V. Riechmann, F. Gao, J. Pielage and the Bloomington, VDRC and NIGfly stock centers and the DSHB for reagents and fly stocks. This work was supported by the Collaborative Research Center CRC1348 (Project B04 to S. Rumpf) and the DFG Excellence cluster EXC 1003 “Cells in Motion”.

References

Arthur, A.L., Yang, S.Z., Abellaneda, A.M., Wildonger, J., 2015. Dendrite arborization requires the dynein cofactor NudE. J. Cell Sci. 128, 2191–2201.
Bentley, M., Banker, G., 2016. The cellular mechanisms that maintain neuronal polarity. Nat. Rev. Neurosci. 17, 611–622.
Bischof, J., Maeda, R.K., Hediger, M., Karch, F., Basler, K., 2007. An optimized transgenesis system for *Drosophila* using germ-line-specific phiC31 integrases. Proc. Natl. Acad. Sci. U. S. A 104, 3312–3317.
Bogard, N., Lan, L., Xu, J., Cohen, R.S., 2007. Rab11 maintains connections between germline stem cells and niche cells in the Drosophila ovary. Development 134, 3413–3418.
Dietzl, G., Chen, D., Schnorrer, F., Su, K.-C., Barinova, Y., Fellner, M., Gasser, B., Kinsey, K., Oppel, S., Scheiblauer, S., Couto, A., Marra, V., Keleman, K., Dickson, B.J., 2007. A genome-wide transgenic RNAi library for conditional gene inactivation in Drosophila. Nature 448, 151–156.
Farias, G.G., Cuitino, L., Guo, X., Ren, X., Jarnik, M., Mattera, R., Bonifacino, J.S., 2012. Signal-mediated, AP-1/clathrin-dependent sorting of transmembrane receptors to the somatodendritic domain of hippocampal neurons. Neuron 75, 810–823.
Ferreira, T.A., Blackman, A.V., Oyrer, J., Jayabal, S., Chung, A.J., Watt, A.J., Sjöström, P.J., van Meyel, D.J., 2014. Neuronal morphometry directly from bitmap images. Nat. Methods 11, 982–984.
Gao, F.B., Brenman, J.E., Jan, L.Y., Jan, Y.N., 1999. Genes regulating dendritic outgrowth, branching, and routing in Drosophila. Genes Dev. 13, 2549–2561.
Gorczyca, D.A., Younger, S., Meltzer, S., Kim, S.E., Cheng, L., Song, W., Lee, H.Y., Jan, L.Y., Jan, Y.N., 2014. Identification of Ppk26, a DEG/ENaC channel functioning with Ppk1 in a mutually dependent manner to guide locomotion behavior in Drosophila. Cell Rep. 9, 1446–1458.
Grueber, W.B., Ye, B., Moore, A.W., Jan, L.Y., Jan, Y.N., 2003. Dendrites of distinct classes of Drosophila sensory neurons show different capacities for homotypic repulsion. Curr. Biol. 13, 618–626.
Grueber, W.B., Ye, B., Yang, C.-H., Younger, S., Borden, K., Jan, L.Y., Jan, Y.-N., 2007. Projections of Drosophila multidendritic neurons in the central nervous system: links with peripheral dendrite morphology. Development 134, 55–64.
Gu, C., Zhou, W., Puthenveedu, M.A., Xu, M., Jan, Y.N., Jan, L.Y., 2006. The microtubule plus-end tracking protein EB1 is required for Kv1 voltage-gated K+ channel axonal targeting. Neuron 52, 803–816.
Guo, Y., Wang, Y., Wang, Q., Wang, Z., 2014. The role of PPK26 in Drosophila larval mechanical nociception. Cell Rep. 9, 1183–1190.
Han, C., Song, Y., Xiao, H., Wang, D., Franc, N.C., Jan, L.Y., Jan, Y.-N., 2014. Epidermal cells are the primary phagocytes in the fragmentation and clearance of degenerating dendrites in Drosophila. Neuron 81, 544–560.
Herzmann, S., Gotzelmann, I., Reekers, L.-F., Rumpf, S., 2018. Spatial regulation of microtubule disruption during dendrite pruning in Drosophila. Development. https://doi.org/10.1242/dev.156950.
Herzmann, S., Krumkamp, R., Rode, S., Kintrup, C., Rumpf, S., 2017. PAR-1 promotes microtubule breakdown during dendrite pruning in Drosophila. EMBO J. 36, 1981–1991.
Hoopfer, E.D., Penton, A., Watts, R.J., Luo, L., 2008. Genomic analysis of Drosophila neuronal remodeling: a role for the RNA-binding protein Boule as a negative regulator of axon pruning. J. Neurosci. 28, 6092–6103.
Issman-Zecharya, N., Schuldiner, O., 2014. The PI3K class III complex promotes axon pruning by downregulating a Ptc-derived signal via endosome-lysosomal degradation. Dev. Cell 31, 461–473.
Kanamori, T., Yoshino, J., Yasunaga, K., Dairyo, Y., Emoto, K., 2015. Local endocytosis triggers dendritic thinning and pruning in Drosophila sensory neurons. Nat. Commun. 6, 6515.
Kirilly, D., Gu, Y., Huang, Y., Wu, Z., Bashirullah, A., Low, B.C., Kolodkin, A.L., Wang, H., Yu, F., 2009. A genetic pathway composed of Sox14 and Mical governs severing of dendrites during pruning. Nat. Neurosci. 12, 1497–1505.
Kuo, C.T., Jan, L.Y., Jan, Y.N., 2005. Dendrite-specific remodeling of Drosophila sensory neurons requires matrix metalloproteases, ubiquitin-proteasome, and ecdysone signaling. Proc. Natl. Acad. Sci. U. S. A 102, 15230–15235.
Lasiecka, Z.M., Winckler, B., 2011. Mechanisms of polarized membrane trafficking in neurons – focusing in on endosomes. Mol. Cell. Neurosci. 48, 278–287.
Lau, C.G., Zukin, R.S., 2007. NMDA receptor trafficking in synaptic plasticity and neuropsychiatric disorders. Nat. Rev. Neurosci. 8, 413–426.
Lee, T., Luo, L., 1999. Mosaic analysis with a repressible cell marker for studies of gene function in neuronal morphogenesis. Neuron 22, 451–461.
Lin, T., Pan, P.-Y., Lai, Y.-T., Chiang, K.-W., Hsieh, H.-L., Wu, Y.-P., Ke, J.-M., Lee, M.-C., Liao, S.-S., Shih, H.-T., Tang, C.-Y., Yang, S.-B., Cheng, H.-C., Wu, J.-T., Jan, Y.-N., Lee, H.-H., 2015. Spindle-F is the central mediator of Ik2 kinase-dependent dendrite pruning in Drosophila sensory neurons. PLoS Genet. 11, e1005642.
Loncle, N., Agromayor, M., Martin-Serrano, J., Williams, D.W., 2015. An ESCRT module is required for neurite pruning. Sci. Rep. 5, 8461.
Loncle, N., Williams, D.W., 2012. An interaction screen identifies headcase as a regulator of large-scale pruning. J. Neurosci. 32, 17086–17096.
Matsubara, D., Horiuchi, S.-Y., Shimono, K., Usui, T., Uemura, T., 2011. The seven-pass transmembrane cadherin Flamingo controls dendritic self-avoidance via its binding to a LIM domain protein, Espinas, in Drosophila sensory neurons. Genes Dev. 25, 1982–1996.

Mauthner, S.E., Hwang, R.Y., Lewis, A.H., Xiao, Q., Tsubouchi, A., Wang, Y., Honjo, K., Skene, J.H., Grandl, J., Tracey, W.D., 2014. Balboa binds to pickpocket in vivo and is required for mechanical nociception in Drosophila larvae. Curr. Biol. 24, 2920–2925.
Meijering, E., Jacob, M., Sarria, J.-C.F., Steiner, P., Hirling, H., Unser, M., 2004. Design and validation of a tool for neurite tracing and analysis in fluorescence microscopy images. Cytom. Part J. 58, 167–176.
Otani, T., Oshima, K., Onishi, S., Takeda, M., Shinmyozu, K., Yonemura, S., Hayashi, S., 2011. IKKepsilon regulates cell elongation through recycling endosome shuttling. Dev. Cell 20, 219–232.
Ritter, A.R., Beckstead, R.B., 2010. Sox14 is required for transcriptional and developmental responses to 20-hydroxyecdysone at the onset of drosophila metamorphosis. Dev. Dynam. 239, 2685–2694.
Rode, S., Ohm, H., Anhäuser, L., Wagner, M., Rosing, M., Deng, X., Sin, O., Leidel, S.A., Storkebaum, E., Rentmeister, A., Zhu, S., Rumpf, S., 2018. Differential requirement for translation initiation factors during ecdysone-dependent neuronal remodeling in Drosophila. Cell Rep. 24, 2287–2299.
Rumpf, S., Bagley, J.A., Thompson-Peer, K.L., Zhu, S., Gorczyca, D., Beckstead, R.B., Jan, L.Y., Jan, Y.N., 2014. Drosophila Valosin-Containing Protein is required for dendrite pruning through a regulatory role in mRNA metabolism. Proc. Natl. Acad. Sci. U. S. A 111, 7331–7336.
Satoh, D., Sato, D., Tsuyama, T., Saito, M., Ohkura, H., Rolls, M.M., Ishikawa, F., Uemura, T., 2008. Spatial control of branching within dendritic arbors by dynein-dependent transport of Rab5-endosomes. Nat. Cell Biol. 10, 1164–1171.
Schindelin, J., Arganda-Carreras, I., Frise, E., Kaynig, V., Longair, M., Pietzsch, T., Preibisch, S., Rueden, C., Saalfeld, S., Schmid, B., Tinevez, J.Y., White, D.J., Hartenstein, V., Eliceiri, K., Tomancak, P., Cardona, A., 2012. Fiji: an open-source platform for biological-image analysis. Nat. Methods 9, 676–682.
Schuldiner, O., Yaron, A., 2015. Mechanisms of developmental neurite pruning. Cell. Mol. Life Sci. 72, 101–119.
Sweeney, N.T., Brenman, J.E., Jan, Y.N., Gao, F.-B., 2006. The coiled-coil protein shrub controls neuronal morphogenesis in Drosophila. Curr. Biol. 16, 1006–1011.
Wang, Q., Wang, Y., Yu, F., 2018. Yif1 associates with Yip1 on Golgi and regulates dendrite pruning in sensory neurons during Drosophila metamorphosis. Development 145 pii: dev164475.
Wang, Y., Zhang, H., Shi, M., Liou, Y.-C., Lu, L., Yu, F., 2017. Sec71 functions as a GEF for the small GTPase Arf1 to govern dendrite pruning of Drosophila sensory neurons. Development 144, 1851–1862.
Welz, T., Wellbourne-Wood, J., Kerkhoff, E., 2014. Orchestration of cell surface proteins by Rab11. Trends Cell Biol. 24, 407–415.
Williams, D.W., Truman, J.W., 2005. Cellular mechanisms of dendrite pruning in Drosophila: insights from in vivo time-lapse of remodeling dendritic arborizing sensory neurons. Development 132, 3631–3642.
Ye, B., Zhang, Y., Song, W., Younger, S.H., Jan, L.Y., Jan, Y.N., 2007. Growing dendrites and axons differ in their reliance on the secretory pathway. Cell 130, 717–729.
Zhang, H., Wang, Y., Wong, J.J.L., Lim, K.-L., Liou, Y.-C., Wang, H., Yu, F., 2014. Endocytic pathways downregulate the L1-type cell adhesion molecule neuroglian to promote dendrite pruning in Drosophila. Dev. Cell 30, 463–478.
Zheng, Y., Wildonger, J., Ye, B., Zhang, Y., Kita, A., Younger, S.H., Zimmerman, S., Jan, L.Y., Jan, Y.N., 2008. Dynein is required for polarized dendritic transport and uniform microtubule orientation in axons. Nat. Cell Biol. 10, 1172–1180.
Zong, W., Wang, Y., Tang, Q., Zhang, H., Yu, F., 2018. Prd1 associates with with the clathrin adaptor α-Adaptin and the kinesin-3 Imac/Unc-104 to govern dendrite pruning in Drosophila. PLoS Biol. 16, e2004506.